AIMS Mathematics, 11(4): 8903–8925.
DOI: 10.3934/math.2026367
Received: 01 February 2026
Revised: 11 March 2026
Accepted: 17 March 2026
Published: 01 April 2026

https://www.aimspress.com/journal/Math

Research article

Nonlinear dynamics and intelligent control of a novel 4D chaotic monetary model with expectation index using SRBF neural networks for sustainable economic stability

Muhamad Deni Johansyah[1,*], Bob Foster[2], Yulian Zifar Ayustira[3], Rameshbabu Ramar[4], Seyed Mohammad Hamidzadeh[5] and Aceng Sambas[6,7,8]

[1] Department of Mathematics, Universitas Padjadjaran, Jatinangor Sumedang 45363, Indonesia
[2] Faculty of Business and Economics, Universitas Informatika dan Bisnis Indonesia, Bandung 40285, Indonesia
[3] Manager of Macroprudential Policy Department, Bank Indonesia, Jakarta 10350, Indonesia
[4] Department of Electronics and Communication Engineering, V. S. B. Engineering College, Karur, Tamilnadu 639111, India
[5] Department of Electrical Engineering, Ferdowsi University of Mashhad, Mashhad 9177948974, Iran
[6] Artificial Intelligence Research Centre for Islam Sustainability (AIRIS), Universiti Sultan Zainal Abidin, Gongbadak, Terengganu 21300, Malaysia
[7] Department of Mathematical Sciences, Saveetha School of Engineering, SIMATS, Chennai, Tamilnadu 602105, India
[8] Department of Mechanical Engineering, Universitas Muhamadiyah Tasikmalaya, Tamansari Gobras, 46196, Tasikmalaya, Indonesia

* **Correspondence:** Email: muhamad.deni@unpad.ac.id.

Abstract: In this paper, we proposed and analyzed a novel chaotic monetary model by extending Lazureanu's three-dimensional economic system through the introduction of a fourth state variable, the Expectation Index (E_i), which captures psychological and behavioral dynamics in financial decision-making. The modified system exhibits rich dynamical features such as chaos, multistability, coexisting attractors, and complex bifurcation behavior. Key parameters influencing chaotic regimes were investigated through bifurcation diagrams and Lyapunov exponent spectra. Furthermore, the model's behavior was controlled using amplitude scaling and DC offset boosting techniques without altering its chaotic structure. To suppress chaos and achieve stabilization, a Supervised Radial Basis

Function Neural Network (SRBFNN) controller was designed. The SRBFNN was trained using system error signals, achieving extremely low mean squared error (MSE) values: 1.14543×10^{-21}, 1.7698×10^{-21}, 2.38218×10^{-19}, and 6.16987×10^{-20} across the four networks. Simulation results demonstrated that the SRBFNN effectively eliminates chaotic behavior and drives the system toward desired equilibrium states with high accuracy and stability.

Keywords: chaotic monetary model; expectation index; SRBFNN; nonlinear control; economic sustainability
Mathematics Subject Classification: 37D45, 37M10, 68T07, 91B62, 93C10

1. Introduction

In recent decades, the global economy has experienced persistent instability characterized by unpredictable market fluctuations, rapid changes in interest rates, inflation volatility, and heightened sensitivity to investor expectations [1,2]. These phenomena are often triggered or amplified by complex feedback loops between macroeconomic variables and policy interventions [3]. Traditional linear economic models, while effective in stable environments, often fall short in capturing the intricate, nonlinear behavior observed during economic crises or speculative bubbles [4]. The 2008 global financial crisis, the COVID-19-induced recession, and recent inflationary pressures are examples where standard monetary tools failed to fully anticipate or mitigate systemic shocks [5].

This growing complexity highlights the need for mathematical models capable of capturing chaotic dynamics inherent in modern monetary systems [6]. Central banks and policymakers increasingly acknowledge that behavioral expectations, cyclical price patterns, and nonlinear interactions among variables such as interest rate, investment, and price levels play a critical role in shaping macroeconomic outcomes [7]. Modeling these factors using tools from nonlinear dynamics and chaos theory enables deeper insights into how minor changes can lead to disproportionate outcomes, especially under uncertainty [8]. Therefore, developing robust, adaptive models that integrate economic structure and psychological feedback has become essential for effective monetary analysis, prediction, and policy design [9].

In the economic context, controlling a monetary model is essential to ensure stability, predictability, and effective policy implementation within financial systems [10]. Monetary variables such as interest rates, investment demand, and price levels often interact in nonlinear ways, potentially leading to unpredictable and chaotic behavior that can destabilize markets and undermine economic confidence [11]. Without appropriate control mechanisms, such chaotic dynamics may trigger inflationary spirals, credit crises, or investment collapses [12]. By applying intelligent control methods to chaotic monetary models, policymakers and financial institutions can regulate fluctuations, maintain macroeconomic equilibrium, and design more resilient strategies to respond to external shocks [13].

The proposed research aligns with the United Nations Sustainable Development Goals (SDGs), particularly SDG 8 (Decent Work and Economic Growth) and SDG 9 (Industry, Innovation, and Infrastructure) [14–16]. By developing a robust chaotic monetary model integrated with psychological expectation dynamics and controlled through intelligent algorithms such as SRBFNN, this study offers a novel framework for enhancing the predictability and resilience of economic

systems. The ability to model and stabilize complex monetary behavior contributes to more informed financial policy-making, risk mitigation, and economic sustainability, ensuring that monetary environments support stable growth, innovation, and long-term socio-economic well-being [17].

Chaotic behavior in financial and monetary systems has drawn significant attention due to its ability to model unpredictable market phenomena. Bouali [18] pioneered the use of nonlinear dynamics in financial systems, demonstrating how simple models could yield complex chaotic behavior. Lazureanu [19] further developed a three-dimensional quadratic monetary model capturing essential interactions between interest rates, investment, and prices, where chaos emerged under specific parameter conditions. Johansyah et al. [20] extended this idea by introducing fractional-order derivatives into a financial model with profit margins, showing that fractional dynamics increase realism and model complexity. Qayyum et al. [21] proposed an optimal control approach using the He-Laplace algorithm for a four-dimensional fractional chaotic finance system, enhancing stabilization. Asadollahi et al. [22] designed fixed-time terminal sliding mode controllers to ensure fast convergence in chaotic economic models. Cheng et al. [23] employed deep reinforcement learning for chaos synchronization, demonstrating AI's potential in controlling nonlinear systems. Liu et al. [24] utilized spiking neural networks to predict chaotic time series, while Syed et al. [25] proposed neuro-stochastic Bayesian networks for financial chaos modeling. Despite these advances, few models integrate psychological expectations and intelligent machine learning control simultaneously. In this study, we address that gap by proposing a four-dimensional chaotic monetary model with an Expectation Index and stabilization via SRBFNN, aiming for enhanced economic predictability and sustainability.

The main contribution and novelty of this paper are as follows:

a. We propose a new four-dimensional chaotic monetary system by extending Lazureanu's model with the inclusion of an E_i to capture behavioral and psychological feedback in financial dynamics.

b. The proposed system is analyzed using bifurcation diagrams and Lyapunov exponent spectra, revealing complex phenomena such as chaos, multistability, coexisting attractors, offset boosting, and amplitude control, which provide deeper insight into the sensitivity and stability of monetary systems.

c. The SRBFNN controller is designed and trained to suppress chaotic behavior in the proposed system. The controller demonstrates high accuracy with extremely low mean squared error values, showcasing its effectiveness in stabilization.

The remainder of this paper is structured as follows: In Section 2, we present the formulation of the proposed chaotic monetary model by extending Lazureanu's three-dimensional system with the inclusion of the E_i, along with the mathematical description of its nonlinear dynamics. In Section 3, a detailed dynamical analysis is conducted through bifurcation diagrams and Lyapunov exponent spectra to identify chaotic regimes and parameter sensitivities. In Section 4, we explore multistability and the coexistence of attractors under varying initial conditions, while in Section 5, we discuss offset boosting and amplitude control techniques to manipulate the system's behavior without altering its chaotic nature. In Section 6, we introduce the design and implementation of a SRBFNN controller for chaos suppression, including training performance and stability results. Finally, in Section 7, we conclude the paper with a summary of key findings, implications for economic modeling, and directions for future research.

2. Mathematical model of monetary model

Lazureanu [19] described an autonomous system of quadratic ordinary differential equations model with monetary system

$$\begin{cases} \dot{I}_r = -aI_r + P_e + I_r I_d + bI_d P_e \\ \dot{I}_d = -cI_d + 1 - I_r^2 \\ \dot{P}_e = -I_r - P_e - bI_r I_d \end{cases} \tag{1}$$

where the state variables I_r, $I_d, P_e \in$ R are interest rate, investment demand, and price exponent, respectively. With a = 0.5; b = -2; c = 0.1; and system (1) observed a chaotic attractor for the monetary system (1) with the initial values $I_r(0) = 0.1, I_d(0) = 0.1$, and $P_e(0) = 0.1$.

To represent the psychological effects and expectations of economic factors that influence the dynamics of the monetary system, the system is modified by adding a fourth variable.

$$\begin{cases} \dot{I}_r = -aI_r + P_e + I_r I_d + bI_d P_e + d_1 E_i \\ \dot{I}_d = -cI_d + 1 - I_r^2 + d_2 E_i \\ \dot{P}_e = -I_r - P_e - bI_r I_d + d_3 E_i \\ \dot{E}_i = -d_4 E_1 + d_5 P_e I_d - d_6 \sin(P_e) \end{cases} \tag{2}$$

where E_i denotes the Expectation Index. Parameters d_1, d_2, and d_3 are E_i sensitivity to interest rate, investment, and price dynamics, d_4 is E_i decay rate (self-regulation), d_5 is the effect of interaction between interest rates and investment on E_i, and d_6 is contribution of the cyclical component of prices to E_i.

The fourth equation governing the Ei captures the dynamic influence of economic and psychological factors on market sentiment. The term −d4 Ei represents the natural decay of expectations over time, reflecting how optimism or pessimism fades in the absence of reinforcing stimuli. The nonlinear term +d5·IdPe models the reinforcement of expectations through the interaction of interest rates and investment demand; when both are active, market participants perceive a strengthening economy, boosting confidence. Moreover, the −d6·sin(Pe) term introduces cyclical volatility, simulating the destabilizing effects of fluctuating price levels (inflation or deflation) on expectations.

The incorporation of the Expectation Index (Ei) in the proposed model is also motivated by the growing literature in behavioral finance and behavioral macroeconomics, which emphasizes the role of psychological expectations and investor sentiment in shaping macroeconomic dynamics. In real financial systems, economic agents often form expectations based not only on objective information but also on subjective perceptions, market sentiment, and feedback from economic fluctuations. Such expectation-driven dynamics can amplify nonlinear interactions between interest rates, investment, and price levels, potentially leading to instability and chaotic behavior. By integrating the Ei variable into the monetary model, the proposed framework aims to capture these behavioral feedback mechanisms, enabling the system to better reflect the complex interaction between economic fundamentals and expectation-driven market responses.

For the simulation of the Novel 4D Chaotic Monetary System with Expectation Index

(N4DCMS-E_i), the parameters are chosen as follows to ensure the system exhibits chaotic behavior: a=0.5, b=−2, and c=0.1 are retained from the original Lazureanu model, while the newly introduced parameters are set to $d_1 = 0.2$, $d_2 = 0.1$, $d_3 = -0.15$, $d_4 = 0.3$, $d_5 = 0.4$, and $d_6 = 0.25$. These values are selected to balance the influence of the Expectation Index on the system's dynamics and maintain the nonlinearity and sensitivity to initial conditions. The initial state of the system is set as $I_r(0) = 0.1$, $I_d(0) = 0.1$, $P_e(0) = 0.1$, and $E_i(0) = 0.05$, representing a low but positive starting level for all variables to simulate the emergence and evolution of chaotic economic dynamics. The Lyapunov exponent (LE) values of the proposed N4DCMS-Ei (2) are calculated using the Wolf algorithm, as given below:

$$(LE_1, LE_2, LE_3, LE_4) = (0.016845, 0, -0.228031, -1.212518)$$

Since the N4DCMS-Ei (2) has only one positive exponent value (LE1 = 0.01685), it is classified as a chaotic model. Figure 1 shows the phase portraits of the proposed N4DCMS-Ei (2).

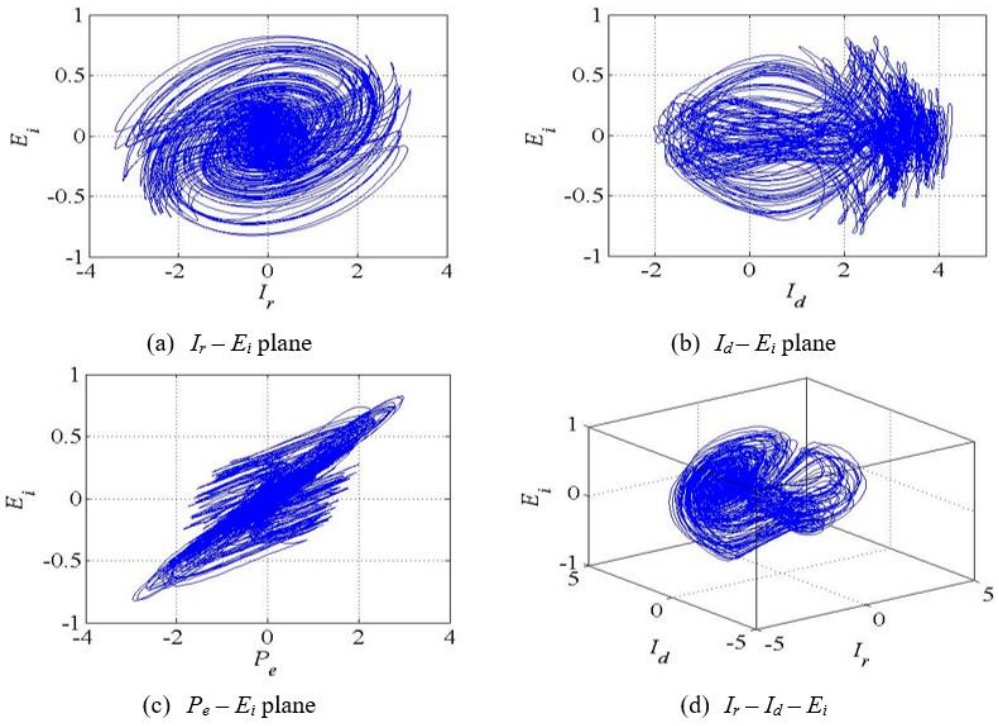

Figure 1. Phase portrait of N4DCMS-E_i (2).

3. Dynamical analysis

In this section, we investigate the complex dynamics of the newly proposed chaotic finance model using bifurcation and LE spectra diagrams. A bifurcation plot uncovers the critical points where the system behaviors changes dramatically when the system parameter varies [26,27]. The bifurcation illustrates the transition between stable and unstable behavior, as well as periodic and chaotic regimes. These provide deep understanding of sensitivity and predictability of the chaotic finance system. The Lyapunov exponent analysis is another powerful technique that not only helps to identify the chaotic regimes but also plays an important role to understand the structural complexity

of dynamical systems. A positive value of LE in the LE spectrum confirms the presence of chaos in the finance system. In this section, all the bifurcation diagram and LE spectrum are plotted by using the initial conditions (0.1, 0.1, 0.1, 0.05) while varying the specific bifurcation parameters against the state Ir.

The bifurcation plot of the new system is shown in Figure 2(a), where the state variable Ir is plotted for continuously increasing parameter a. Figure 2(a) reveals that the system has strange attractors from $a = 0$ to $a = 0.95$ as indicated by the dense and cloud of points within this interval. As the parameter a increases beyond $a = 0.95$, a noticeable change in the system response is observed. The system transitions to periodic nature as evidenced by the appearance of separated branches and a single line. The corresponding Lyapunov spectrum, as shown in Figure 2(b) further supports the findings in the bifurcation plot. The positive LE1 (shown in Blue) in the interval $a = 0$ to $a = 0.95$ is a defining feature of chaos. For $a > 0.95$, LE drops to zero and stabilizes at zero aligning with the visual evidence of periodic nature in the bifurcation plot.

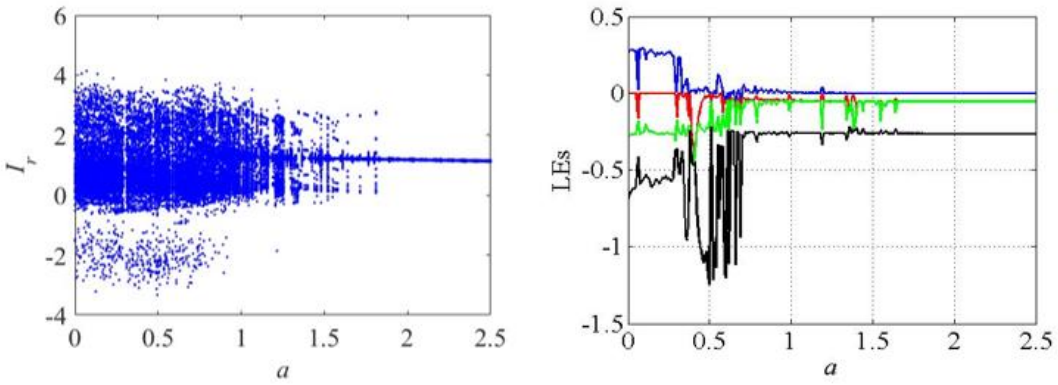

(a) Bifurcation diagram (b) Lyapunov exponent plot

Figure 2. (a) Bifurcation diagram and (b) LEs as the function of a.

The bifurcation plot and its corresponding LE spectrum for the function of parameter b are given in Figure 3(a) and Figure 3(b), respectively. As observed from Figure (3a), the system has chaotic regime for the region $b = 0$ to $b = 3.5$, except for few smaller regions where periodic behavior emerges. The existence of chaotic region is evidenced by the dense and scattered distribution of state variable points. However, there exist several narrow intervals where the system changes into periodic regimes. The corresponding LE spectrum, as given in Figure 3(b), further supports the observation made from the bifurcation plot. A positive LE1 over most of the parameter region confirms the presence of chaos in the system. Conversely, the system momentarily its chaotic behavior in the small regions where the LE1 approaches zero and LE2 (shown in Red) becomes negative, aligning with the periodic regions observed in the bifurcation plot.

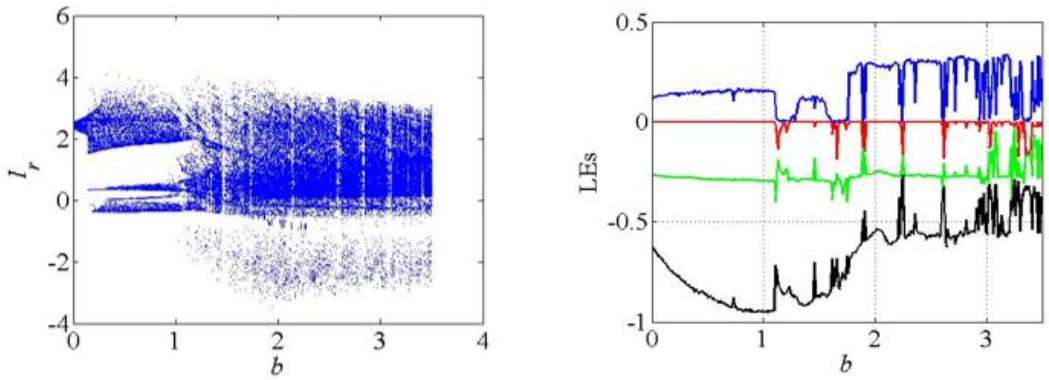

(a) Bifurcation diagram (b) Lyapunov exponent plot

Figure 3. (a) Bifurcation diagram and (b) LEs as the function of b.

Figure 4 depicts the bifurcation plot and its corresponding LE spectrum of the system as bifurcation parameter c varies gradually in the range $0 \le c \le 0.4$. Figure 4(a), the bifurcation plot of the system, shows that the system has chaotic dynamics when the parameter lies in the interval $c = 0$ to $c = 0.15$. As parameter c increases beyond $c = 0.15$, the system changes from chaos to periodic, and settles into stable fixed points. Figure 4(b) provides further validation of the observed behavior through the LE spectrum. The LE1 remains positive within the interval $c = 0$ to $c = 0.15$, confirming the presence of chaotic behavior in the system. As c increases beyond $c = 0.15$, the LE1 gradually decreases and stabilizes in to zero, indicating the loss of chaotic behavior and onset of periodic behavior in the system.

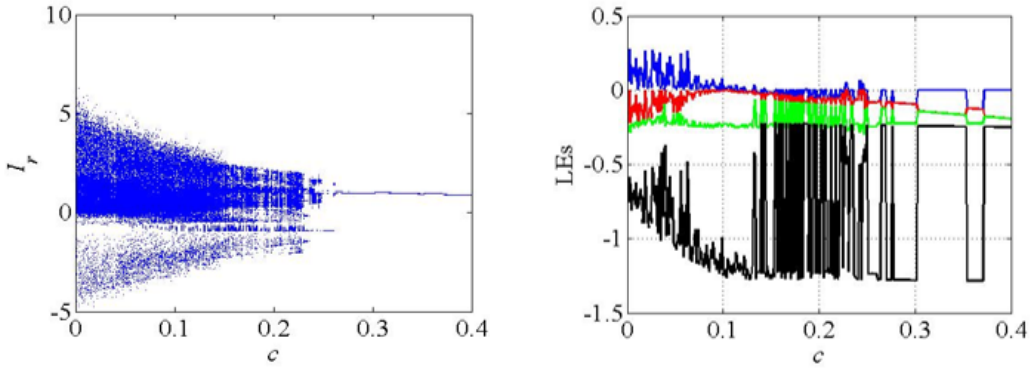

(a) Bifurcation diagram (b) Lyapunov exponent plot

Figure 4. (a) Bifurcation diagram and (b) LE spectrum as the function of c.

Figure 5 depicts the bifurcation plot and LE spectrum with respect to parameter d_1 against the state variable I_r. Figure 5(a) shows the bifurcation plot, while Figure 5(b) shows the variation of LEs over the same parameter interval. It can be observed from Figure 5a that the system exhibits chaotic behavior in the parameter interval $d_1 = 0$ to $d_1 = 1.5$, identified by the existence of dense and cloud of scattered points. The absence of regular and repeating patterns in this region reveals that the system does not settle in to fixed stable points. Beyond $d_1 = 1.5$, the system transitions into successive periodic and stable points, as evidenced by the repetitive structure and single lines. The

corresponding LE spectrum serves as the quantitative verification of the chaotic region noted in the bifurcation plot. A positive LE1 in the interval $d_1 = 0$ to $d_1 = 1.5$ confirms the existence of chaos in the system. As the parameter increases beyond $d_1 = 1.5$, the LE1 stabilizes at zero, indicating the transition into periodic behavior.

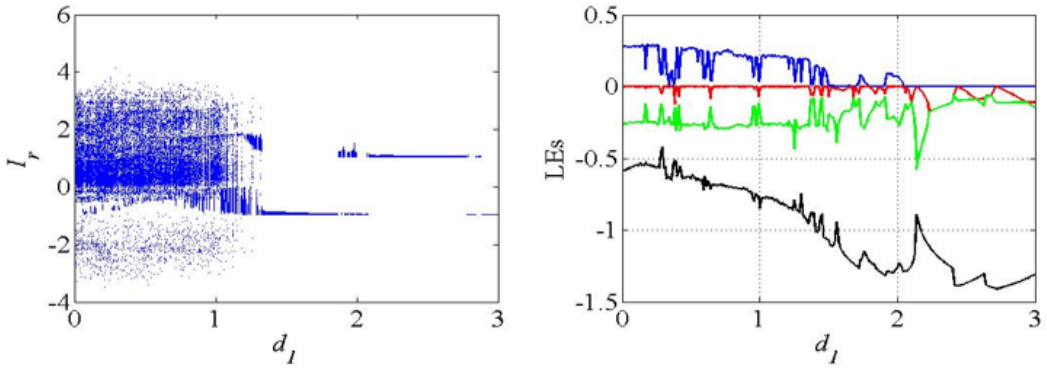

(a) Bifurcation diagram (b) Lyapunov exponent plot

Figure 5. (a) Bifurcation diagram and (b) LE spectrum as the function of d_1.

Figure 6(a) shows the bifurcation plot of the system as the function of the bifurcation parameter d_5, where the state variable Ir is plotted in vertical axis. It is evident from Figure 6(a) that the system exhibits successive chaotic and periodic behavior as parameter d_5 gradually increases from $d_5 = 0$ to $d_5 = 3$. Particularly, the state variable I_r displays the irregular and densely populated points within the parameter range $d_5 = 0$ to $d_5 = 1.5$, which is the indicator of chaotic attractors in the system. Beyond d5=1.5, the system has sparsely populated points and branches of a single line, indicating the periodic regions where the system settles into stable fixed points. The LE spectrum for parameter d_5 is shown in Figure 6(b), where the presence of positive LE1 within the interval $d_5 = 0$ to $d_5 = 1.5$ holds the chaotic nature, whereas the zero LE1 in the interval $d_5 = 1.6$ to $d_5 = 3$ indicates the periodic and stable behavior of the system.

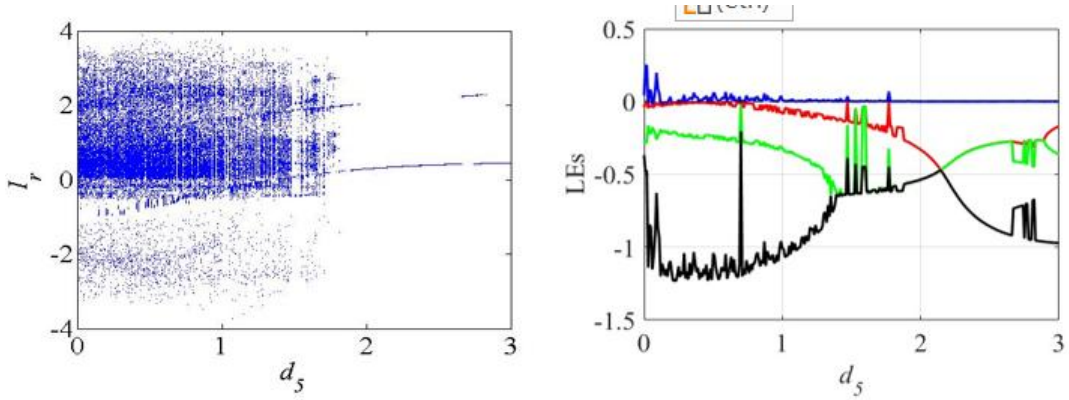

(a) Bifurcation diagram (b) Lyapunov exponent plot

Figure 6. (a) Bifurcation diagram and (b) LE spectrum as the function of d_5.

4. Multistability and coexisting attractors analysis

Multistability is the nonlinear phenomenon where multiple attractors coexist under a different set of initial conditions and the same set of parameters. In such a multistable system, the state of the system is highly dependent on the initial conditions of state variables. This behavior leads to diverse dynamical responses such as chaotic trajectories, periodic motion, and stable points. To observe the multistability in the proposed system, a detailed numerical analysis is carried out by plotting the bifurcation diagram. For each initial condition, the trajectory of the system is plotted with sufficient transient time, and the corresponding attractor is plotted in the phase space. The results show the presence of multistability and coexisting attractors for the same set of parameters.

For example, the bifurcations for the parameter d_1 are plotted with the two sets of initial conditions as given in Figure 7. In Figure 7, the branches in blue and red color correspond to the initial condition (0.1, 0.1, 0.1, 0.05), and (-0.1, -0.1, -0.1, 0.05), respectively. The non-overlapping regions in Figure 8 confirm the presence of multiple attractors for the same parameter value, indicating multistability. In contrast, the overlapped regions suggest the existence of the single attractors at those parameter values.

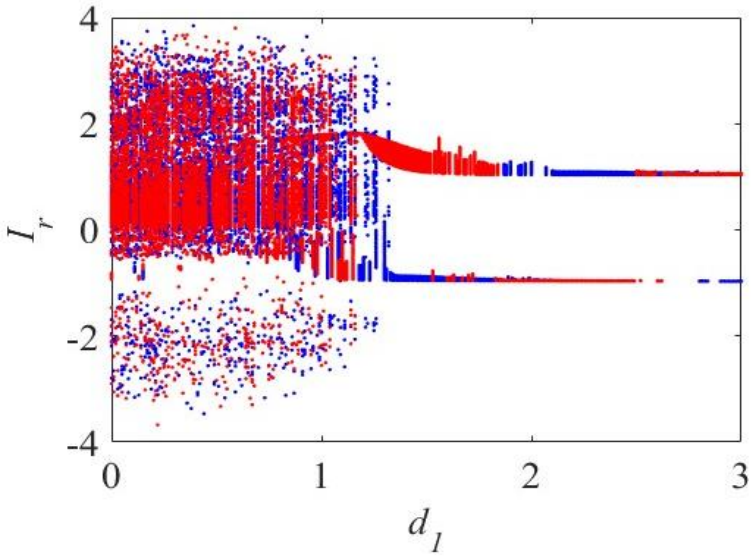

Figure 7. Bifurcation plots under the initial conditions (0.1, 0.1, 0.1, 0.05) (Blue), and (-0.1, -0.1, -0.1, 0.05) (red).

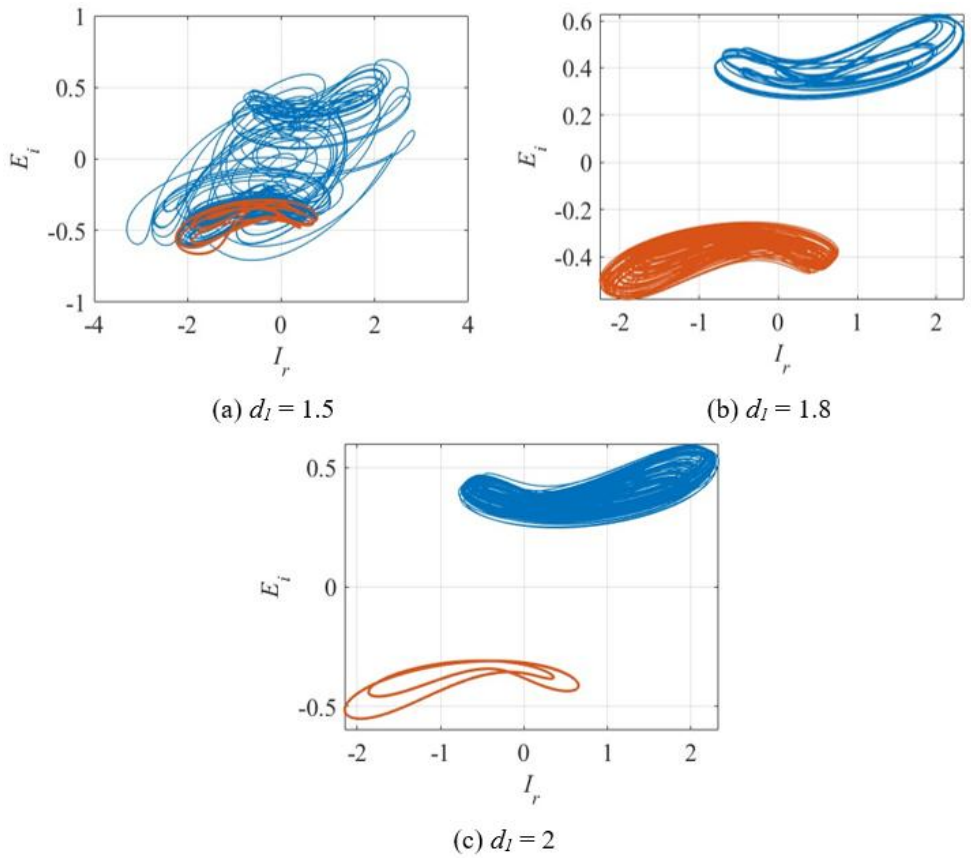

Figure 8. Various coexisting attractors of the proposed system under different initial conditions. (a) Periodic coexisting attractor $d_1 = 1.5$, (b) and (c) Mixed periodic and chaotic coexisting attractors at $d_1 = 1.8$ and $d_1 = 2$, respectively.

5. Offset boosting analysis and amplitude control

Dc offset boosting in a chaotic system refers to a method to shift its attractor's position in phase space without altering its chaos and bifurcation structure [28]. This can be achieved by the intentional addition of a constant booster parameter to the state variables of the system. It is an important technique often used for signal control and transformation. For example, it changes the negative chaotic signal to positive to meet the input range of Analog to Digital converter or Digital to Analog Converter, and is used in chaotic modulation where the specific voltage levels are required. The offset boosting can be analyzed by plotting an attractor diagram, bifurcation diagram and LE spectrum for various booster parameters. The attractor boostable system is given in the Eq (3), where B is the booster parameter. Since the system has multiple E_i signals on the right side of the equation, booster parameter B is added to each E_i, which shifts the location of the state signal E_i in phase space without disturbing the location of the remaining state signals.

$$\begin{cases} \dot{I}_r = -aI_r + P_e + I_r I_d - bI_d P_e + d_1(E_i + B) \\ \dot{I}_d = -cI_d + 1 - I_r^2 + d_2(E_i + B) \\ \dot{P}_e = -I_r - P_e + bI_r I_d - d_3(E_i + B) \\ \dot{E}_i = d_5 I_d P_e - d_6 \sin(P_e) - d_4(E_i + B) \end{cases} \tag{3}$$

Figure 9 shows the offset transformation of the system with the different booster values B = 0, (blue), B = 2 (red), and B = -2 (black). For B = 0, the Ei signal retains its original positive, and is considered as a reference. As the booster parameter is set as B = 2, the signal is shifted on downward direction along the state signal Ei. When B = -2, the signal moves upward, showing a negative offset in the system.

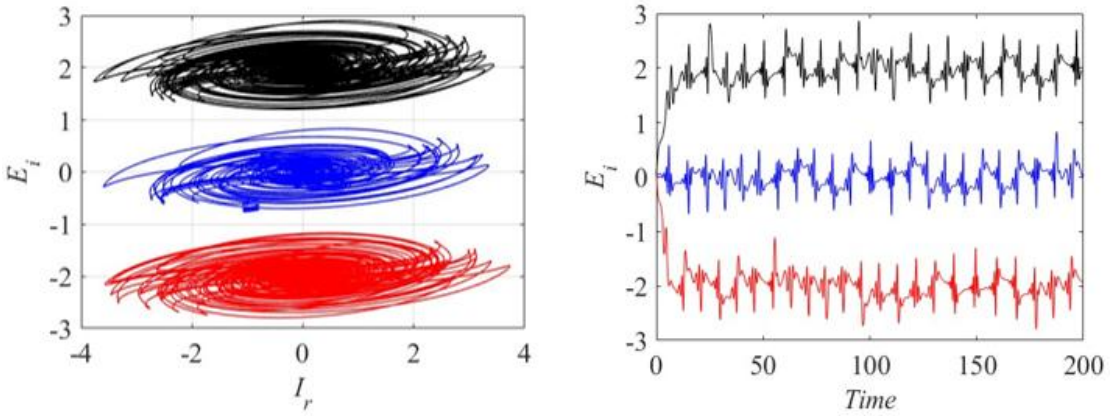

(a) Offset boosted attractors (b) Time series of E_i

Figure 9. Influence of the offset booster parameter. (a) Offset boosted attractors along the E_i state signals, and (b) the time variation of the signal E_i with booster parameters

Figure 10(a) displays the corresponding bifurcation plots against the state variable Ei with the same booster values. This indicates that the positive value of B moves the bifurcation branch in a downward direction, whereas the negative value of B moves the branches in upward direction. These results confirm that the booster parameter effectively controls the location of state signals without affecting its chaotic dynamics and bifurcation structure. The offset boosting directly affects the average (mean) value of the state signal Ei. This effect is illustrated in Figure 10(b), which displays the plot of average values of the state variables against the booster parameter B. As shown in the Figure 10(b), the mean value of Ei gradually decreases as the booster parameter increases, while the remaining states variables are unchanged.

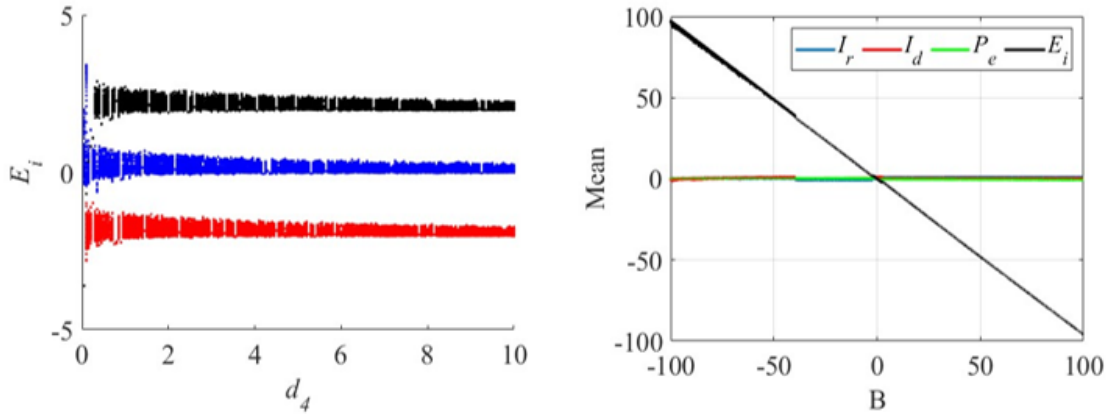

(a) Bifurcation plots (b) Mean plot

Figure 10. (a) The bifurcation plots against E_i state signals with different booster values, and (b) the variation of the mean value for the state signals with respect to booster value.

In many physical systems, the chaotic oscillations increase its magnitude in uncontrolled manner and lead to system instability. The amplitude control mechanism keeps the chaotic trajectories within bounded limits [29–31]. It enables their practical use in a wide range of practical applications such as a chaotic communication system [32–34]. Rescaling the state variables is one of the easiest and efficient methods to achieve the amplitude control. The original state variables of the system can be transformed into new variables by multiplying them by a constant parameter. Now, let us take $I_r \to \alpha I_r, I_d \to \alpha I_d, P_e \to \alpha P_e, E_i \to \alpha E_i$, and the proposed N4DCMS-Ei (2) becomes amplitude controllable system, as given in Eq (4), where α is the amplitude control parameter.

$$\begin{cases} \dot{I}_r = -aI_r + P_e + \alpha I_r I_d - \alpha b I_d P_e + d_1 E_i \\ \dot{I}_d = -cI_d + \alpha^{-1} - \alpha I_r^2 + d_2 E_i \\ \dot{P}_e = -I_r - P_e + \alpha b I_r I_d - d_3 E_i \\ \dot{E}_i = \alpha d_5 I_d P_e - \alpha^{-1} d_6 \sin(\alpha P_e) - d_4 E_i \end{cases} \tag{4}$$

Figure 11 displays the amplitude-controlled attractor of the new system under the control parameters $\alpha = 1(\text{blue}), \alpha = 0.7(\text{red})$, and $\alpha = 1.4(\text{green})$, As evident from Figure 11, that the controller adjusts the amplitude of the chaotic signal by the factor $\frac{1}{\alpha}$. This means that the amplitude of the signal is amplified when $\alpha \prec 1$ and attenuated when $\alpha \succ 1$, without affecting its chaotic dynamics. In conclusion, the proposed control method effectively regulates the amplitude of the chaotic signal without modifying its dynamics.

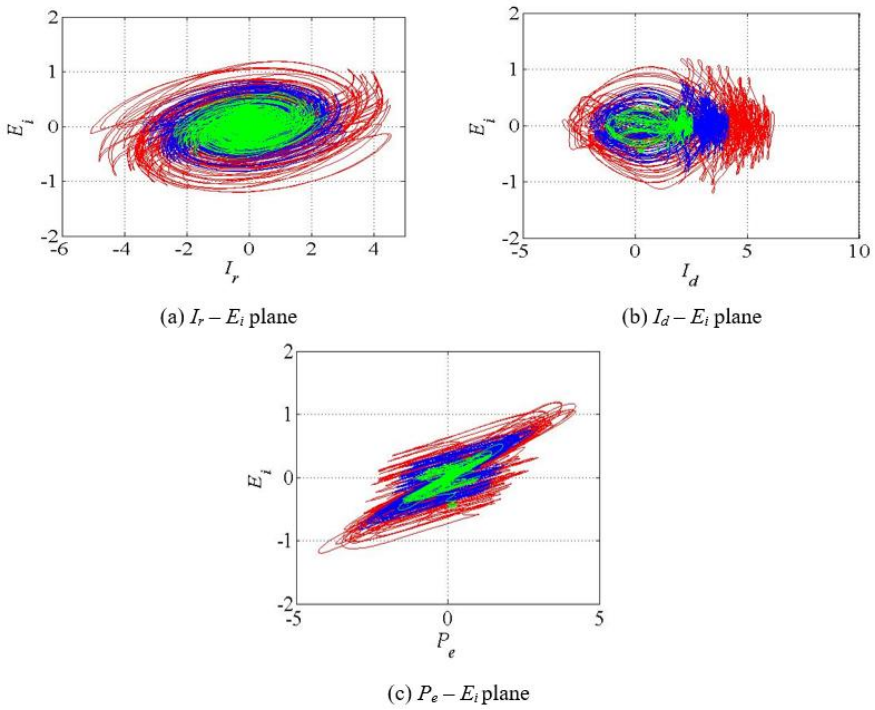

Figure 11. The amplitude regulated attractors of the new system under the control parameters $\alpha = 1(\text{blue}), \alpha = 0.7(\text{red})$, and $\alpha = 1.4(\text{green})$.

6. Supervised radial basis function neural network

In this section, the design method of a supervised radial descending function neural network controller is presented. In this method, the radial descending function neural network is first trained with data. This data is obtained using a nonlinear design method.

$$\begin{cases} \dot{I}_r = -aI_r + P_e + I_r I_d + bI_d P_e + d_1 E_i + U_{1-NL} \\ \dot{I}_d = -cI_d + 1 - I_r^2 + d_2 E_i + U_{2-NL} \\ \dot{P}_e = -I_r - P_e - bI_r I_d + d_3 E_i + U_{3-NL} \\ \dot{E}_i = -d_4 E_i + d_5 I_d P_e - d_6 \sin(P_e) + U_{4-NL} \end{cases} \tag{5}$$

In the Eq (5), $U_{1-NL}, U_{2-NL}, U_{3-NL}$, and U_{4-NL} are controllers that need to be designed.

In other words, the error data and the error derivative are used as the input of the network, and the controller data are used as the correct response of the network. This means that the radial descent function neural network can learn the inherent behavior of the nonlinear controller.

$$\begin{aligned} e_{I_r} &= I_r - I_r^* \\ e_{I_d} &= I_d - I_d^* \\ e_{P_e} &= P_e - P_e^* \\ e_{Ei} &= E_i - E_i^* \end{aligned} \tag{6}$$

Taking the time derivative of the error variables yields

$$\begin{aligned} \dot{e}_{I_r} &= \dot{I}_r - \dot{I}_r^* \\ \dot{e}_{I_d} &= \dot{I}_d - \dot{I}_d^* \\ \dot{e}_{P_e} &= \dot{P}_e - \dot{P}_e^* \\ \dot{e}_{E_i} &= \dot{E}_i - \dot{E}_i^* \end{aligned} \tag{7}$$

Since I_r^*, I_d^*, P_e^*, and E_i^* are constant equilibrium values, their derivatives are zero. Therefore, the error derivatives are given as above.

$$\begin{aligned} \dot{e}_{I_r} &= \dot{I}_r \\ \dot{e}_{I_d} &= \dot{I}_d \\ \dot{e}_{P_e} &= \dot{P}_e \\ \dot{e}_{E_i} &= \dot{E}_i \end{aligned} \tag{8}$$

Theorem 1. The system (8) with free initial conditions moves exponentially toward the desired points if the nonlinear controllers are as follows:

$$\begin{aligned} U_{1-NL} &= -aI_r - P_e - I_r I_d - bI_d P_e - d_1 E_i + \lambda_1 e_{I_r} \\ U_{2-NL} &= cI_d - 1 + I_r^2 - d_2 E_i + \lambda_2 e_{I_d} \\ U_{3-NL} &= I_r + P_e + bI_r I_d - d_3 E_i + \lambda_3 e_{P_e} \\ U_{4-NL} &= d_4 E_i - d_5 I_d P_e + d_6 \sin(P_e) + \lambda_4 e_{E_i} \end{aligned} \tag{9}$$

where $\lambda_1, \lambda_2, \lambda_3,$ and λ_4 are the control gains of Eq (9). These parameters are positive constants that determine the convergence rate of the error dynamics. According to the Lyapunov stability condition, choosing λi > 0 ensures that the derivative of the Lyapunov function is negative definite, which guarantees the asymptotic stability of the controlled system.

Proof 1: By the candidate Lyapunov function:

$$V(e) = \frac{1}{2}(e_{I_r}^2 + e_{I_d}^2 + e_{P_e}^2 + e_{E_i}^2) > 0\,. \tag{10}$$

By the derivative from the candidate Lyapunov Eq (10):

$$\dot{V} = \dot{e}_1 e_1 + \dot{e}_2 e_2 + \dot{e}_3 e_3\,. \tag{11}$$

By substituting Eq (9) in Eq (11):

$$\dot{V} = \lambda_1 e_{I_r}^2 + \lambda_2 e_{I_d}^2 + \lambda_3 e_{P_e}^2 + \lambda_4 e_{E_1}^2 < 0 \qquad (\lambda_1 = \lambda_2 =, \lambda_3 = \lambda_4 < 0). \tag{12}$$

It is noted that the desired points are equal to $I_r^* = I_d^* = P_e^* = E_i^* = 0$. The proof is now complete.

In the numerical simulation for the Eq (5), the initial conditions are equal to I_r (0) = 0.1, I_d (0) = 0.1, P_e (0) = 0.1, and E_i (0) = 0.05, and the system parameters are equal to d_1 = 0.2, d_2 = 0.1, d_3 = −0.15, d_4 = 0.3, d_5 = 0.4, d_6 = 0.25, a = 0.5, b = −2, and c = 0.1. Additionally, the controller gain is equal to $\lambda_1 = \lambda_2 =, \lambda_3 = \lambda_4 = -3$. Figure 12 depicts the behavior of the Eq (5) before and after applying the nonlinear controller. Figure 13 show the time response of nonlinear controller.

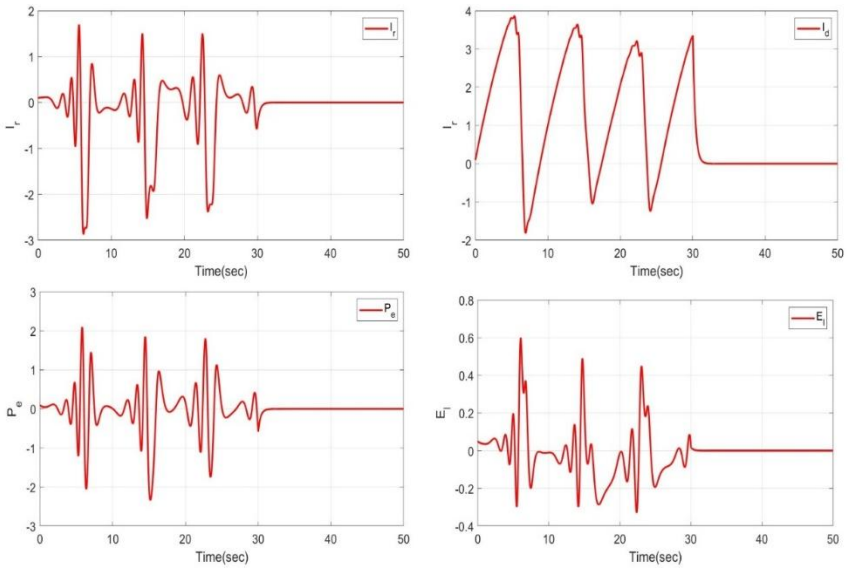

Figure 12. Time response of a chaotic monetary system before and after applying a nonlinear controller.

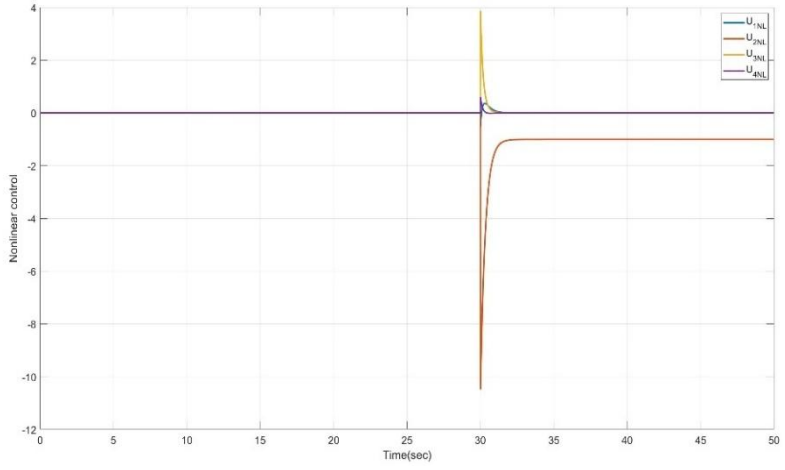

Figure 13. Time response of nonlinear controller.

In chaotic systems, there is a complex relationship between variables. The strength of the proposed method is the use of four error variables for training simultaneously. This means that the radial descent function neural network controller has four inputs and one output and this design method helps the neural network to be robust. Therefore, four radial descent function neural networks are designed (due to four controllers). Figure 14 shows the block diagram of training a supervised radial basis function neural network.

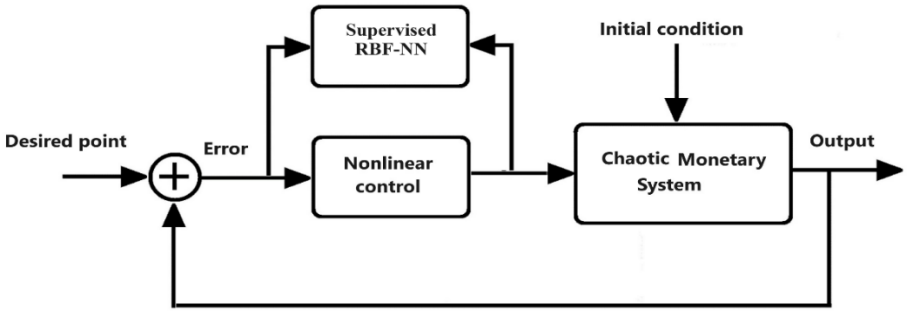

Figure 14. Block diagram of the SRBFNN training system.

In the design of the neural network controller, the supervised radial basis function Eq (5) changes as follows:

$$\begin{cases} \dot{I}_r = -aI_r + P_e + I_r I_d + bI_d P_e + d_1 E_i + U_{1-RBF} \\ \dot{I}_d = -cI_d + 1 - I_r^2 + d_2 E_i + U_{2-RBF} \\ \dot{P}_e = -I_r - P_e - bI_r I_d + d_3 E_i + U_{3-RBF} \\ \dot{E}_i = -d_4 E_i + d_5 I_d P_e - d_6 \sin(P_e) + U_{4-RBF} \end{cases} \tag{13}$$

where $U_{1-RBF}, U_{2-RBF}, U_{3-RBF}$, and U_{4-RBF} are controllers SRBFNN to be designed.

The way data is selected for training neural networks is very important. In this method, training data is selected from Time = 30 sec to Time = 32.5 sec. This interval is selected because the chaotic system has already reached a fully developed chaotic regime after the transient phase. Therefore, the system trajectories within this period contain representative nonlinear dynamics of the chaotic attractor, which are sufficient for the SRBFNN to learn the nonlinear characteristics required for the control design. This structure is given in Table 1. Additionally, Table 2 shows the mean square error for training. Figure 15 shows the output results of the radial basis function neural network.

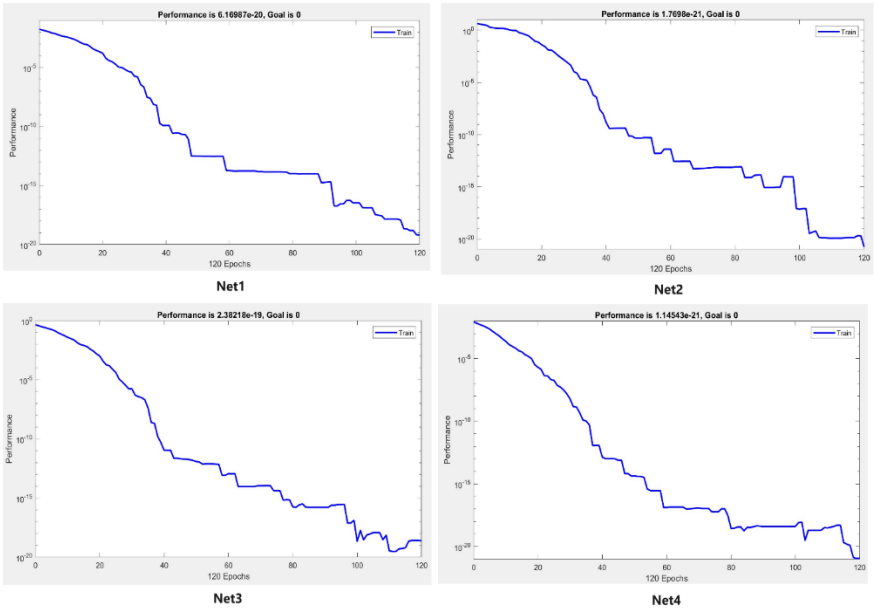

Figure 15. Performance of training the proposed SRBF-NN controller.

Table 1 Description of RBFNN architecture.

RBF parameters	Number
Total number of trainings	225
Number of training pairs	113
Number of test pairs	112
Mean squared error goal (P1)	0
Spread of radial basis functions (P2)	0.1
Maximum number of neurons (P3)	200
Number of neurons to add between displays (P4)	30
Epoch (7)	120

Table 2. MSE training.

	Net1	Net2	Net3	Net4
Parameter	E1, E2, E3 E4 and U1	E1, E2, E3 E4 and U1	E1, E2, E3 E4 and U1	E1, E2, E3 E4 and U1
MSE	1.14543e-21	2.38218e-19	1.7698e-21	6.16987e-20

This trained network will be used for online deployment in the chaotic monetary system. This means solving Eq (13) under the SRBFNN controller. The block diagram of the chaotic monetary system under the SRBFNN controller can be seen in Figure 16.

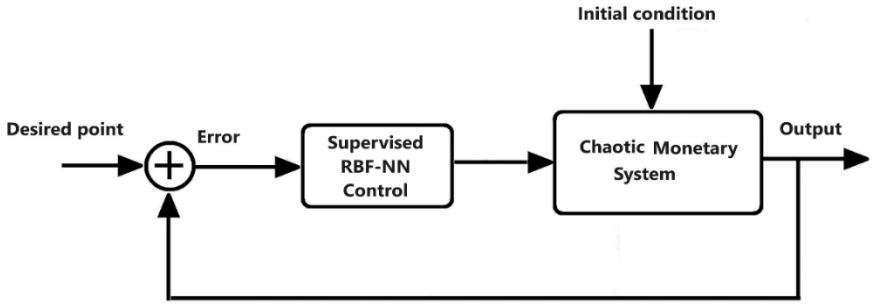

Figure 16. Block diagram of chaotic monetary system under the SRBFNN controller.

Simulation results for the radial basis function neural network controller will be described in this section. The initial conditions are equal to I_r (0) = 0.1, I_d (0) = 0.1, P_e (0) = 0.1, and E_i (0) = 0.05, and the system parameters are equal to $d_1 = 0.2$, $d_2 = 0.1$, $d_3 = -0.15$, $d_4 = 0.3$, $d_5 = 0.4$, $d_6 = 0.25$, $a = 0.5$, $b = -2$, and $c = 0.1$. Changing the initial conditions in chaotic systems will change their behavior. This can be a good measure to evaluate the performance of the controller. Additionally, the time of application of the SRBFNN controller has also changed compared to what was in training.

As can be seen in Figure 17, the SRBFNN controller has been applied to the chaotic monetary system since time t = 38. The stability time and elimination of chaotic behavior show that the proposed controller has an acceptable performance. Additionally, Figure 18 depicts the behavior of the radial basis function neural network controller. This behavior represents the implementation of the controller structure in the real world.

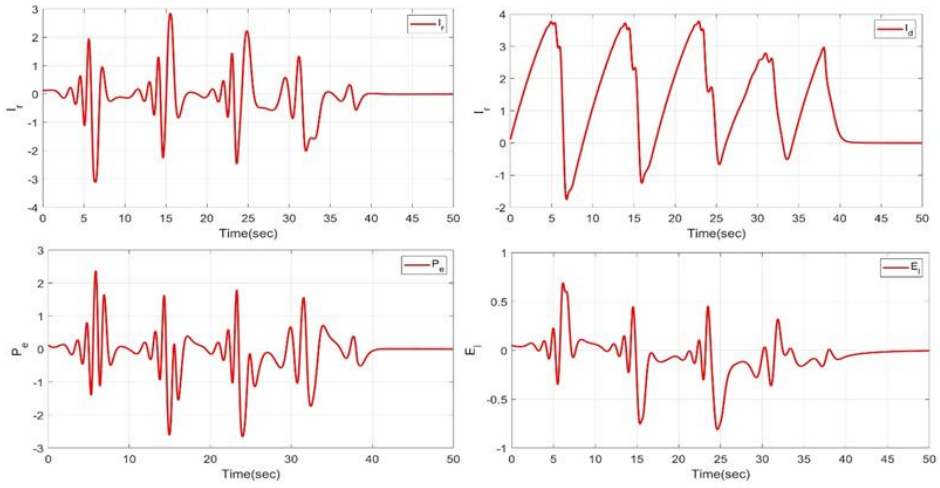

Figure 17. Time response of a chaotic monetary system under a SRBFNN controller.

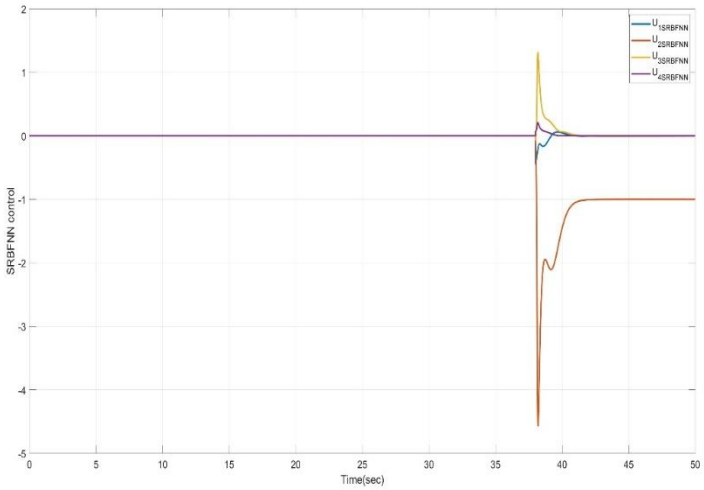

Figure 18. Time response of a SRBFNN controller.

Although the effectiveness of the proposed SRBFNN controller has been demonstrated through numerical simulations, further investigations can be conducted in future work. In particular, a comparative analysis with other advanced control strategies, such as sliding mode control and reinforcement learning-based controllers, would provide deeper insights into the convergence performance, robustness, and disturbance rejection capability of the proposed method.

From a practical perspective, the proposed chaotic monetary model provides a conceptual framework for understanding how nonlinear interactions between macroeconomic variables and expectation dynamics may influence financial stability. In real monetary systems, central banks frequently adjust policy instruments such as interest rates and liquidity management to stabilize economic fluctuations. The presence of chaotic dynamics in the model suggests that small parameter changes may lead to significant variations in economic trajectories, highlighting the importance of adaptive and intelligent control strategies. The SRBFNN-based control approach demonstrated in this study illustrates how advanced computational techniques could support decision-making by stabilizing complex economic dynamics and reducing excessive volatility in macroeconomic indicators.

7. Conclusions

In this study, we present a comprehensive framework for understanding and regulating chaotic dynamics in a four-dimensional monetary model enhanced with an E_i. Through extensive dynamical analysis, including bifurcation structures, Lyapunov exponents, and multistability exploration, the model revealed highly sensitive and diverse behaviors influenced by both economic variables and behavioral expectations. The introduction of amplitude control and offset boosting provided additional flexibility for managing the system's response without altering its inherent chaotic nature. Furthermore, the deployment of a SRBFNN demonstrated the effectiveness of intelligent control in driving the system toward equilibrium under varying initial conditions. These findings highlight the practical value of combining nonlinear modeling with machine learning-based control to improve economic system resilience and design adaptive responses to instability.

The proposed framework also contributes to the broader objectives of sustainable development, particularly SDG 8 (Decent Work and Economic Growth) and SDG 9 (Industry, Innovation, and Infrastructure). Stable and predictable monetary environments are essential for promoting sustainable economic growth, encouraging long-term investment, and maintaining financial resilience. By providing a mathematical and computational approach to analyze and control complex monetary dynamics, this study supports the development of innovative analytical tools that can enhance the robustness of economic systems. Such approaches may assist policymakers and financial institutions in designing strategies that mitigate instability while fostering sustainable economic development.

Authors contributions

Muhamad Deni Johansyah: Conceptualization, Data curation, Funding acquisition, Supervision, Writing-original draft; Bob Foster: Data curation, Formal analysis, Funding acquisition, Validation, Writing-review & editing; Yulian Zifar Ayustira: Formal analysis, Validation, Visualization, Writing-review & editing; Rameshbabu Ramar: Investigation, Methodology, Software Resources, Writing-original draft; Seyed Mohammad Hamidzadeh: Investigation, Methodology, Software Resources, Visualization, Writing-original draft; Aceng Sambas: Conceptualization, Supervision. All authors have read and approved the final version of the manuscript for publication.

Use of Generative-AI tools declaration

The authors declare that they have not used Artificial Intelligence (AI) tools in the creation of this article.

Acknowledgements

The authors sincerely thank the anonymous reviewers who have helped to improve the paper.

Funding

This research was funded by the Directorate of Research and Innovation Funding, Deputy for Research and Innovation Facilities, and the National Research and Innovation Agency of the Republic of Indonesia together with Padjadjaran University through the Research and Innovation Program for Advanced Indonesia Competition IX scheme with contract numbers 212/IV/KS/10/2025 and 3653a/UN6.3.1/PT.00/2025.

Availability of data and material

No data was used for the research described in the article.

Conflict of interest

The authors declare that they have no known competing financial interests or personal relationships that could have appeared to influence the work reported in this paper.

References

1. B. Gaies, Exploring the time-varying predictability of global financial instability over the last two decades: the influence of climate change news, *J. Econ. Stud.*, **52** (2025), 904–918. https://doi.org/10.1108/JES-01-2024-0031
2. T. L. Yang, F. X. Zhou, M. Du, Q. Y. Du, S. R. Zhou, Fluctuation in the global oil market, stock market volatility, and economic policy uncertainty: A study of the US and China, *Q. Rev. Econ. Financ.*, **87** (2023), 377–387. https://doi.org/10.1016/j.qref.2021.08.006
3. M. A. Shahmi, Interaction of macroeconomic variable shocks and monetary policy interventions on the profitability of sharia commercial banks in Indonesia, *Imara: Jurnal Riset Ekonomi Islam*, **7** (2023), 11–19. https://doi.org/10.31958/imara.v7i1.9360
4. Y. Liu, X. Zhao, Y. Liu, F. J. Kong, The dynamic impact of digital economy on the green development of traditional manufacturing industry: evidence from China, *Econ. Anal. Policy*, **80** (2023), 143–160. https://doi.org/10.1016/j.eap.2023.08.005
5. W. Hynes, B. D. Trump, P. Love, A. Kirman, S. E. Galaitsi, G. Ramos, et al., Resilient financial systems can soften the next global financial crisis, *Challenge*, **63** (2020), 311–318. https://doi.org/10.1080/05775132.2020.1822660
6. S. Mohammadi, S. R. Hejazi, H. Saeidi, G. ElahiShirvan. Modeling and optimal control of nonlinear fractional order chaotic system of factors affecting money laundering: genetic algorithms and particle swarm optimization, *Appl. Econ.*, **57** (2025), 3092–3113. https://doi.org/10.1080/00036846.2024.2333713
7. M. A. Khan, H. Ali, H. Shabbir, F. Noor, M. D. Majid, M. Atif, Impact of macroeconomic indicators on stock market predictions: A cross-country analysis, *Journal of Computing & Biomedical Informatics*, **8** (2024), 1–13.
8. K. Shaurav, A. Deheri, B. N. Rath, Understanding corruption in India: determinants, nonlinear dynamics and policy implications, *Int. J. Emerg. Mark.*, **20** (2025), 3315–3341. https://doi.org/10.1108/IJOEM-08-2023-1273
9. Q. L. Chen, Z. Sabir, M. Umar, H. M. Baskonus, A Bayesian regularization radial basis neural network novel procedure for the fractional economic and environmental system, *Int. J. Comput. Math.*, **102** (2025), 280–291. https://doi.org/10.1080/00207160.2024.2409794
10. L. Q. Dinh, T. T. K. Oanh, N. T. H. Ha, Financial stability and sustainable development: perspectives from fiscal and monetary policy, *Int. J. Financ. Econ.*, **30** (2025), 1724–1741. https://doi.org/10.1002/ijfe.2981
11. S. Mohammadi, S. R. Hejazi, H, Saeidi, G. ElahiShirvan, Modeling and optimal control of nonlinear fractional order chaotic system of factors affecting money laundering: genetic algorithms and particle swarm optimization, *Appl. Econ.*, **57** (2025), 3092–3113. https://doi.org/10.1080/00036846.2024.2333713
12. D. Schäfer, W. Semmler, Is interest rate hiking a recipe for missing several goals of monetary policy—beating inflation, preserving financial stability, and keeping up output growth, *Eurasian Econ. Rev.*, **14** (2024), 235–254. https://doi.org/10.1007/s40822-023-00256-6
13. H. El Ouazzani, H. Ouakil, A. Moustabchir, A simulation of the macroeconomic effects of the Russia–Ukraine War on the Moroccan economy using the DSGE model, *Afr. Dev. Rev.*, **36** (2024), S75–S93. https://doi.org/10.1111/1467-8268.12726

14. J. W. Liu, L. Ji, Y. A. Sun, Y. H. Chiu, H. X. Zhao, Unleashing the convergence between SDG 9 and SDG 8 towards pursuing SDGs: Evidence from two urban agglomerations in China during the 13th five-year plan, *J. Clean. Prod.*, **434** (2024), 139924. https://doi.org/10.1016/j.jclepro.2023.139924
15. K. M. A. Aziz, A. O. Daoud, A. K. Singh, M. Alhusban, Integrating digital mapping technologies in urban development: Advancing sustainable and resilient infrastructure for SDG 9 achievement–a systematic review, *Alex. Eng. J.*, **116** (2025), 512–524. https://doi.org/10.1016/j.aej.2024.12.078
16. N. Amin, A. Sharif, M. Tayyab, Y. C. Pan, Green technological advances and resource rents as levers for carbon reduction in BRICS: implications for SDGs 7, 8, 9, 12, and 13, *Sustain. Dev.*, **33** (2025), 3171–3195. https://doi.org/10.1002/sd.3294
17. S. Mariappanadar, Improving quality of work for positive health: interaction of sustainable development goal (SDG) 8 and SDG 3 from the sustainable HRM perspective, *Sustainability*, **16** (2024), 5356. https://doi.org/10.3390/su16135356
18. S. Bouali, The hunt hypothesis and the dividend policy of the firm. The chaotic motion of the profits, *8th International Conference of the Society for Computational Economics Computing in Economics and Finance*, Aixen Provence, France, 2002, 27–29.
19. C. Lazureanu, Chaotic behavior of an integrable deformation of a nonlinear monetary system. *AIP Conf. Proc.*, **2116** (2019), 370004. https://doi.org/10.1063/1.5114377
20. M. D. Johansyah, A. Sambas, S. Qureshi, S. Zheng, T. M. Abed-Elhameed, S. Vaidyanathan, et al., Investigation of the hyperchaos and control in the fractional order financial system with profit margin, *Partial Differential Equations in Applied Mathematics*, **9** (2024), 100612. https://doi.org/10.1016/j.padiff.2023.100612
21. M. Qayyum, E. Ahmad, S. T. Saeed, A. Akgül, S. M. El Din, New solutions of fractional 4D chaotic financial model with optimal control via He-Laplace algorithm, *Ain Shams Eng. J.*, **15** (2024), 102503. https://doi.org/10.1016/j.asej.2023.102503
22. M. Asadollahi, N. Padar, A. Fathollahzadeh, M. J. Mirzaei, E. Aslmostafa, Fixed-time terminal sliding mode control with arbitrary convergence time for a class of chaotic systems applied to a nonlinear finance model, *Int. J. Dynam. Control*, **12** (2024), 1874–1887. https://doi.org/10.1007/s40435-023-01319-x
23. H. X. Cheng, H. H. Li, Q. L. Dai, J. Z. Yang, A deep reinforcement learning method to control chaos synchronization between two identical chaotic systems, *Chaos Soliton. Fract.*, **174** (2023), 113809. https://doi.org/10.1016/j.chaos.2023.113809
24. Q. Liu, H. Peng, L. F. Long, J. Wang, Q. Yang, M. J. Pérez-Jiménez, et al., Nonlinear spiking neural systems with autapses for predicting chaotic time series, *IEEE T. Cybernetics*, **54** (2024), 1841–1853. https://doi.org/10.1109/TCYB.2023.3270873
25. F. A. Syed, K. T. Fang, A. K. Kiani, M. Shoaib, M. A. Z. Raja, Design of Neuro-Stochastic bayesian networks for nonlinear chaotic differential systems in financial mathematics, *Comput. Econ.*, **65** (2025), 241–270. https://doi.org/10.1007/s10614-024-10587-4
26. S. Gao, R. Wu, X. Y. Wang, J. F. Liu, Q. Li, C. P. Wang, et al., Asynchronous updating Boolean network encryption algorithm, *IEEE T. Circ. Syst. Vid.*, **33** (2023), 4388–4400. https://doi.org/10.1109/TCSVT.2023.3237136

27. S. Gao, R. Wu, H. H. C. Iu, U. Erkan, Y. H. Cao, Q. Li, et al., Chaos-based video encryption techniques: A review, *Comput. Sci. Rev.*, **58** (2025), 100816. https://doi.org/10.1016/j.cosrev.2025.100816
28. S. Gao, H. H. C. Iu, U. Erkan, C. Simsek, A. Toktas, Y. H. Cao, et al., A 3D memristive cubic map with dual discrete memristors: design, implementation, and application in image encryption, *IEEE T. Circ. Syst. Vid.*, **35** (2025), 7706–7718. https://doi.org/10.1109/TCSVT.2025.3545868
29. Q. Lai, C. K. Zhu, X. W. Zhao, X. Sun, J. L. Hua, A unified framework for generating 4-D discrete memristive hyperchaotic maps with complex dynamics and application to encryption, *IEEE Internet Things*, **12** (2025), 40934–40943. https://doi.org/10.1109/JIOT.2025.3590465
30. Q. Lai, H. Q. Hua, L. Yang, Encryption design and analysis of 3-D medical models in internet of medical things using a novel memristive hyperchaotic map, *IEEE Internet Things*, **12** (2025), 39019–39028. https://doi.org/10.1109/JIOT.2025.3587815
31. Q. Lai, J. Wang, D. X. Huang, Diverse dynamical behaviors and predefined-time synchronization of a simple memristive chaotic system, *Acta Phys. Sin.*, **74** (2025), 200501. https://doi.org/10.7498/aps.74.20250954
32. F. Yu, X. X. Kong, W. Yao, J. Zhang, S. Cai, H. R. Lin, et al., Dynamics analysis, synchronization and FPGA implementation of multiscroll Hopfield neural networks with non-polynomial memristor, *Chaos Soliton. Fract.*, **179** (2024), 114440. https://doi.org/10.1016/j.chaos.2023.114440
33. T. He, F. Yu, Y. Lin, S. Q. He, W. Yao, S. Cai, et al., Multi-scroll hopfield neural network excited by memristive self-synapses and its application in image encryption, *Chin. Phys. B.*, **34** (2025), 120506. https://doi.org/10.1088/1674-1056/adfeff
34. W. Feng, Z. X. Tang, X. Y. Zhao, Z. T. Qin, Y. Chen, B. Cai, et al., State-dependent variable fractional-order hyperchaotic dynamics in a coupled quadratic map: A novel system for high-performance image protection, *Fractal Fract.*, **9** (2025), 792. https://doi.org/10.3390/fractalfract9120792

AIMS Press

© 2026 the Author(s), licensee AIMS Press. This is an open access article distributed under the terms of the Creative Commons Attribution License (https://creativecommons.org/licenses/by/4.0)